International Journal of Engineering & Technology, 7 (3.29) (2018) 597-603

International Journal of Engineering & Technology

Website: www.sciencepubco.com/index.php/IJET

Research paper



Performance comparison between ZSI and SL-ZSI based axial flux permanent magnet synchronous generator wind energy conversion system for different wind speeds with different PWM methods

V. Ramesh babu [1] *, J. Srinivasa rao [1], M. Ranjit [2], S. Vijayarama rao [3]

[1] *Associate Professor*
[2] *Assistant Professor*
[3] *PG student*
**Corresponding author E-mail: rameshbabu0506@gmail.com*

Abstract

In this paper the performance comparison between Impedance source Inverter (ZSI) and Switched Inductor Impedance Source Inverter(SL ZSI)based Axial Flux Permanent Magnet Synchronous Generator(AFPMSG) wind energy conversion system for different wind speeds with different PWM methods are discussed. The generator generates different voltage values for different wind speeds. The Switched Inductor Z-Source Inverter performance is analyzed for various voltage values of AFPMSG. This is done to predict suitable inverter and to reduce the conversion stages of the Wind Energy Conversion System. For comparison analysis voltage gain, Switching stress and Total Harmonic Distortion (THD) are taken into consideration. Axial Flux Permanent Magnet Machines are characterized by the short axial length and high power to weight ratio and hence these machines facilitate direct compact integration with the wind turbine, The key features like high efficiency, high power density, elimination of gearbox and fast dynamic response make this kind of machines very attractive for Wind application. By connecting more number of inductors and diodes to the Z-Source inverter bridge, multi cell Switched Inductor Z-Source Inverter is formed, and it can boost voltage nearly two times more than conventional ZSI with the same shoot through duty ratio. Hence the switching stress on the Z capacitors and Inverter bridge get reduced. Thus, the proposed topology require less power electronic switches, and more reliable under short circuit. The simulation readings are compared for different wind speeds and for all three PWM methods to identify which is the best PWM method for SL ZSI.

Keywords: *Wind Energy Conversion System (WECS); Axial Flux Permanent Magnet Synchronous Generator (AFPMSG); Switched Inductor Z-Source Inverter (SL ZSI); Simple Boost PWM; Maximum Constant PWM and Maximum Constant Boost PWM using THI.*

1. Introduction

The conventional energy resources like coal, gas etc are getting depleted continuously due to the rapid increase in energy demand i.e two to three times every year, especially in developing county like India. Alternatively, the entire world looking towards the use of renewable energy resources like solar, wind and fossil fuels. The use of wind energy intensified in 1970 and it is drastically increasing. The wind is the most plentiful renewable energy source and numerous techniques exist to transform wind energy into electrical energy. The use of wind energy makes the environment pollution free. As the running cost comes down with windmills installed, the WES attracts the attention worldwide.

Permanent Magnet machine is the fastest growing research topic for many research fellows because of its special features like as high power density, high efficiency, high torque to weight ratio and very advantageous for variable speed drive applications. According to Air gap flux direction PMSG are classified into two types one is Radial Flux machines and another type is Axial Flux machines. The principle of operation of both the machines is same but differ in construction [2] [3]. In Axial flux machines, the Air gap flux direction is in Axial direction and the effective current carrying conductors are radially constructed. In conventional constant speed wind energy conversion system having a gearbox to make the speed of Wind turbine and Generator be same. The gearbox is always associated with high fatigue, noise and high maintenance requirements, complexity in their control [1]. By using AFPMSG we can eliminate the gearbox because Axial flux permanent magnet synchronous machine having a large number of poles so it makes shaft speed same with the turbine blades.

We have two types of inverters Voltage Source Inverter (VSI) and Current Source Inverter (CSI) having problems like Shoot through problem (Triggering of two switches in the same limb at a time), limited output voltage (either lesser or greater than input voltage), main circuit can't be interchanged (either Buck or Boost operation) and higher harmonic distortion due to dead time and overlap time. To overcome these problems a new type of inverter was proposed by F. Z. pang in 2003[4] called as ZSI.

The most widely used conventional WECS uses a three-stage power conversion i.e, Rectification, DC-DC boosting up and PWM based inversion to obtain the desired output voltage. In this work, we can reduce the number of conversion stages by using a Z-Source inverter. The Z-Source can boost the voltage and can control the maximum power point and hence we can eliminate the DC-DC boost

Copyright © 2018 V. Ramesh babu et. al. This is an open access article distributed under the Creative Commons Attribution License, which permits unrestricted use, distribution, and reproduction in any medium, provided the original work is properly cited.

converter stage. Some of the advantages of the Z-Source Inverter are (1). Due to its shoot-through states handling ability, its application is more reliable. (2). Lower cost and less size than a conventional converter (inductors and capacitors can be optimally designed). (3). More effective than an ordinary inverter.
The main drawback with Z-Source Inverter is that it requires high voltage Z-Capacitor to perform voltage boost action which further increases the volume and cost. The initial voltage across the Z-Source capacitor is '0', so a huge inrush current charges the capacitor instantly to half the input voltage, then the resonance of Z-Source capacitor and inductor starts, which results in large voltage and current surge which may destroy the device. To eliminate the disadvantages many improved topologies are implemented in Z-Network. In this process, few diodes and inductors are added to form a Switched Inductor Z-Source Inverter (SL-ZSI). The modulation methods that have been developed in the ZSI can be effectively utilized as a part of proposed ZSI. The voltage boost ratio is substantially higher than the standered ZSI under the same shoot-through duty ratio. Furthermore, the proposed ZSI can diminish the voltage stress on Z-source capacitor and inverter-bridge altogether as it requires a smaller shoot-through duty ratio is for high voltage boost.
The proposed ZSI and SL ZSI based Direct Driven WECS are compared with traditional in terms of the voltage gain, Shoot through distribution, switching stress and Total Harmonic Distortion (THD) for different loading condition.

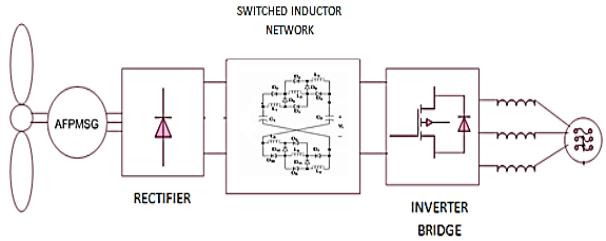


Fig. 1: Block diagram of AFPMSG based WECS with Switched Inductor Z-Source Inverter.

2. Axial flux permanent magnet synchronous generator wind energy conversion system

a) Wind turbine

Basically, wind turbines are classified into two types of a variable speed wind turbine and fixed speed wind turbine. Compared to fixed speed wind turbine, variable speed wind turbine have the more advantages like availability, more efficiency and can operate at the maximum power point.
The power extracted from the wind turbine is given by

$$E = 0.5mv^2 \tag{1}$$

The theoretical maximum power efficiency of any wind turbine is 0.59 (i.e. not more than 59% of the energy carried by the wind can be extracted by a wind turbine). This is known as the "power coefficient" and is characterized as:

$$C_{pmax} = 0.59 \tag{2}$$

The power extracted from the wind turbine is given by

$$P = 0.5\rho A v^3 C_p \tag{3}$$

The modeling of the wind turbine can be done based on below differential equations

$$\frac{d\omega_t}{dt} = \frac{1}{j_t}[T_t(V_w, \omega_t) - T_s]$$

$$\frac{dT_s}{dt} = K_s[\omega_t - \omega_g] + \frac{B_s}{J_t}[T_t(V_w, \omega_t) - T_s] + \frac{B_s}{J_g}[T_g(\cos\alpha, \omega_g) - T_s]$$

$$\frac{d\omega_g}{dt} = \frac{1}{j_g}[T_g - T_s] \tag{4}$$

The generator torque in terms of arbitrary reference frame variables is given as

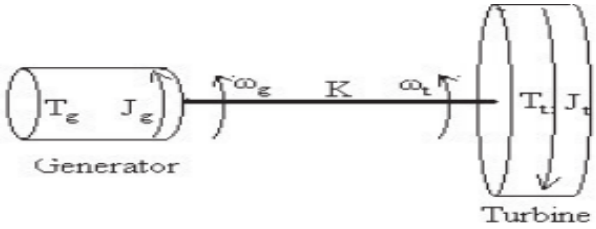


Fig. 2: Torque Interaction Generator and Turbine.

b) Axial Flux Permanent Magnet Synchronous Generator

According to the air gap flux direction permanent magnet machines are classified into two types radial and axial flux permanent magnet machines. The operation of both machines is same but differ in construction, in radial flux machines the current carrying conductors are placed parallel to the shaft axis and the air gap flux is radial to the shaft axis and in Axial flux machines the conductors are placed in radial and air gap flux in axial direction w.r.to shaft axis.
Based on the construction axial flux permanent magnet machines are classified into four types

a) Single Rotor and Single Stator
b) Double Rotor and Single Stator (TORUS)
c) Double stator and Single Rotor (AFIR)
d) Multi Stator and Multi Rotor

The main disadvantage in the single rotor and single stator construction is the strong magnetic pull between stator and rotor, it may bends the rotor disc so to avoid this problem new topology is designed that is the stator is sandwiched between two rotors or the rotor is sandwiched between two stators.
The dynamic modeling of axial flux permanent magnet synchronous generator can be done by converting the simple three phase generator equations into d-q frame. The diagrams shows the equivalent circuits of d and q reference frames assuming the flux linkage of permanent magnetic materials.

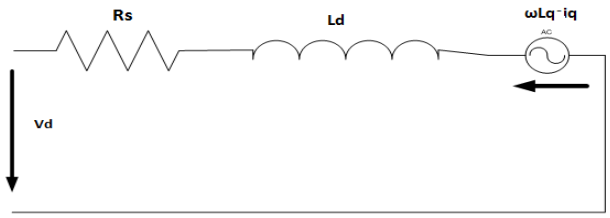


Fig. 3: Direct Axis Model of AFPMG.

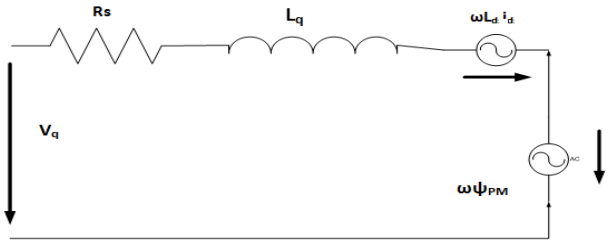


Fig. 4: Quadratic Axis Model of AFPMG.

$$v_d = R_s i_d + L_d \frac{di_d}{dt} - \omega L_q i_q \tag{5}$$

$$v_q = R_s i_q + L_q \frac{di_q}{dt} + \omega L_d i_d + \omega \psi_{PM} \tag{6}$$

The relation between electromagnetic torque and AFPMSG parameters is given by

$$T_e = \frac{3}{2}p(i_d i_q(L_d - L_q) + \psi_f i_q \quad (7)$$

3. Switched inductor Z-source inverter

The conventional VSI has the natural drawbacks like constraint of AC output voltage, the short circuit occurred by miss firing from PWM, and distortion in AC output current because the presence of Dead time in PWM is eliminated by using ZSI.
Z-Source inverter also has the drawbacks like rush current and resonance between Z-network capacitors and Inductors at starting, voltage and current surges and stress on capacitors and inverter bridge, It can be reduced for formation of switched inductor Z-Source inverter, it is important to add some more inductors and diodes to the Z-Network of normal ZSI shown in Fig 5, and it can give a high voltage boost ratio with the same modulation index value which is used in normal ZSI by this we can get high ac output voltage with less stress on capacitors and inverter bridge.

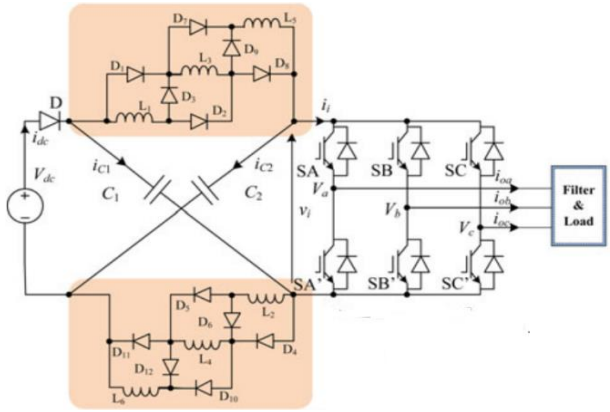


Fig. 5: Switched Inductor Z-Source Inverter.

In this SL-ZSI topology, according to shoot-through state and non-shoot-through state. The arrangement of inductors is changed.
Shoot-through state
Diode (D) is reverse biased, In the upper branch, diodes D1, D2, D3, and D4 are in conduction mode, while two diodes D5 and D6 are in non-conduction mode. Then, by capacitor C1 charges the parallel connected inductors L1, L2, and L3.
In the lower branch, diodes D7, D8, D9, and D10 are in conduction mode, while two diodes D11 and D12 are in non-conduction mode. Then, capacitor C2 charges the parallel connected inductors L4, L5, and L6.
This state forms the additional Zero State of SL-ZSI, this is formed by the shoot-through actions of the top and bottom arms, and its equivalent circuit is shown in Fig 9. It seems that the same function to absorb the energy stored in the capacitors.
Non-shoot-through state (including active and null state)
Diode (D) is forward biased, In the upper branch, diodes D1, D2, D3, and D4 are in the non-conduction mode, while two diodes D5 and D6 are in conduction mode. Then the series connected inductors L1, L2, and L3 are transfer the stored energy to the inverter circuit.
In the lower branch, diodes D7, D8, D9, and D10 are in the non-conduction mode, while two diodes D11 and D12 are in conduction mode. Then the series connected inductors L4, L5, and L6 are transfer the stored energy to the inverter circuit.
To supplement the consumed energy of C_1 and C_2 during the shoot through state C_1 is charged by V_{in} via the bottom SL cell, and C_2 is charged by V_{in} via the top SL cell.

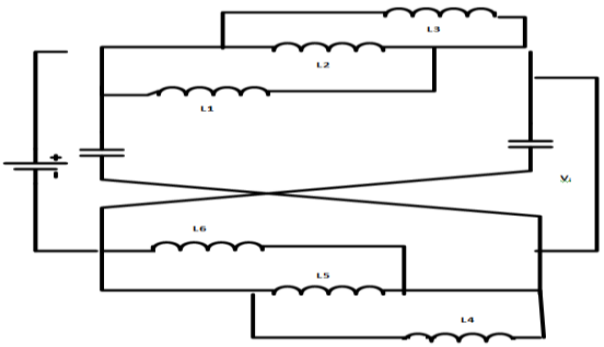


Fig. 6: Shoot Through State of SLZSI.

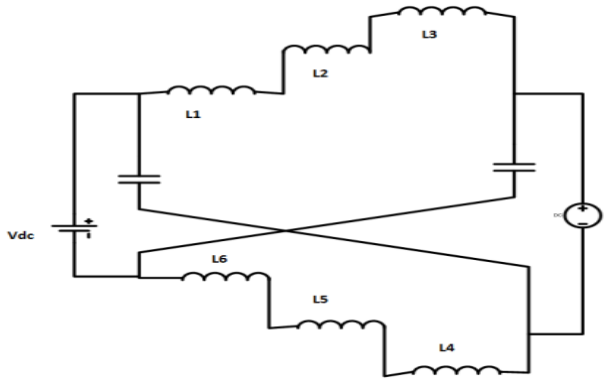


Fig. 7: Non Shoot Through State of SL ZSI.

The network becomes symmetrical, by choosing the same inductance(L) value of six inductors and the same capacitance (C) value of two capacitors. From symmetrical circuit, capacitors and inductor voltages become

$$Vc1=Vc2=Vc \quad (8)$$

$$VL1=VL2=VL3=VL4=VL5=VL6=VL \quad (9)$$

From Shoot through state equivalent circuit

$$VL=VC \quad (10)$$

$$VI=0 \quad (11)$$

From Non-Shoot through state equivalent circuit is shown in the figure the voltage can be expressed as :

$$3V_L = V_{dc} - V_C \quad (12)$$

$$V_i = V_C - 3V_L = 2V_C - V_{dc}$$

From the fact that in a steady state over one switching period average voltage of the inductor should be zero, (13) can be derived by using (12)

$$V_L = v_L = \frac{T_0 V_C + (1-T_0)(\frac{V_{dc}-V_C}{2})}{T} = 0 \quad (13)$$

$$V_C = \frac{1-\alpha}{1-4\alpha} V_{dc} \quad (14)$$

The inverter bridge peak DC-link voltage can be expressed in (13) and can be rewritten:

$$V_i = V_C - 3V_L = 2V_C - V_{dc} = \frac{1+2\alpha}{1-4\alpha} V_{dc} \quad (15)$$

Thus the boost factor B can be obtained by

$$B = \frac{1+2\alpha}{1-4\alpha} \quad (16)$$

The proposed ZSI as Voltage gain is expressed as

$$G = M.B = (1-\alpha)\frac{1+2\alpha}{1-4\alpha} \quad (17)$$

4. Pulse width modulation techniques

4.1. Simple boost pulse width modulation

How Switching Pulses are generated by Simple Boost Pulse Width Modulation technique is shown in the Fig 8. It is almost similar to the Conventional Pulse Width Modulation Technique but differs in a production of shoot through zero states. It consists of three reference waves those are V_a, V_b, and V_c and two DC voltage lines V_p and V_n. At the point when the carrier triangular wave more prominent than the upper DC voltage line Vp or lower than the Lower DC voltage line Vn, the circuit transforms into a shoot through state. Else, it works as a conventional PWM.
This method is simple but it creates high stress across switching devices because of low modulation index.

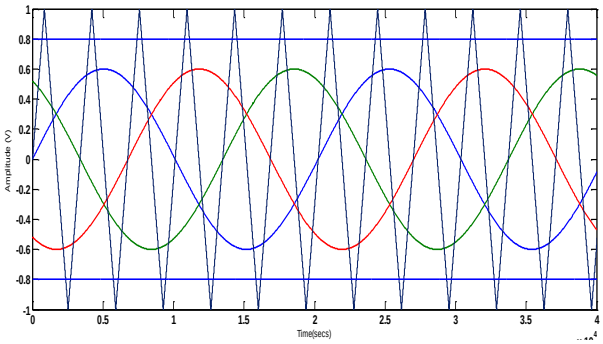


Fig. 8: Simple Boost Pulse Width Modulation.

In Simple Boost PWM, the Boost Factor is given by

$$B = \frac{1}{2M-1} \quad (18)$$

For any boost factor, the modulation Index can be used is

$$M = \frac{B+1}{2B} \quad (19)$$

The Voltage gain of this method is given by

$$G = M.B = \frac{V_{ac}}{\frac{V_{dc}}{2}} = \frac{B+1}{2} \quad (20)$$

4.2. Maximum constant boost PWM

To reduce the stress on the switching devices Maximum Boost PWM technique is introduced but it creates low- frequency current ripple because of Capacitor Voltage and inductor current which increases the passive component requirement.
So cost and volume of the circuit may increases. To reduce the cost and volume, we need to eliminate the low-frequency current ripple it should be possible by utilizing a consistent shoot through duty ratio. In the meantime, a greater voltage boost for any modulation index is desired to reduce the voltage stress across the switches. This can be achieved by using Maximum Constant Boost Pulse Width Modulation. The fundamental point is to get the maximum boost while keeping it consistent all the time is the upper and lower envelopes are periodical and are three times the output frequency.
In this strategy, it comprises of three reference waves Va, Vb and, Vc and two shoots through envelopes Vp and Vn. At the point when the carrier triangular wave more than the upper envelope Vp or lower than the Lower envelope Vn, the circuit transforms into a shoot through state. Else, it works as a conventional PWM. The figure 9 demonstrates the sketch map Maximum Constant Boost PWM.

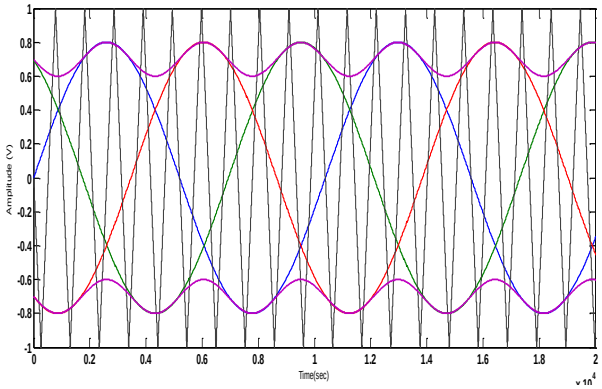


Fig. 9: Maximum Constant Boost PWM.

There are two half periods for both curves in a cycle. For the primary half period (0, Π/3)
The first half-period, the envelop curves are expressed by below equations

$$V_{p1} = \sqrt{3M} + M\sin(\theta - \frac{2\pi}{3}) \text{ For } 0<\theta< 2\Pi/3$$

$$V_{n1} = M\sin(\theta - \frac{2\pi}{3}) \text{ For } 0<\theta< \Pi/3$$

For the second half period (Π/3, 2Π/3), the envelope curves are given as

$$V_{p2} = M\sin(\theta) \text{ For } \Pi/3<\theta< 2\Pi/3$$

$$V_{n2} = M\sin(\theta) - \sqrt{3}\,M \text{ For } \Pi/3<\theta< 2\Pi/3$$

The distance between these two curves can be calculated by shoot through duty ratio is always constant for a given modulation index M that is $\sqrt{3}M$
The shoot through duty ratio can be expressed as

$$D_0 = \frac{2-\sqrt{3}M}{2} \quad (21)$$

The boost factor can be calculated as

$$B = \frac{1}{1-2D_0} = \frac{1}{\sqrt{3}M-1} \quad (22)$$

Therefore the modulation index and voltage gain for maximum constant boost control is given by

$$M = \frac{B+1}{\sqrt{3}B} \quad (23)$$

$$G = M.B = \frac{V_{ac}}{V_{dc}/_2} = \frac{B+1}{\sqrt{3}} \quad (24)$$

But maximum Constant boost PWM produces high harmonic distortion in the output waveform. Third harmonic injection is commonly utilized in inverters is to increase the modulation index range. The third harmonic injection is used here to extent the range of modulation index by which the range of voltage gain increments and at the same time harmonic distortion in the output waveform also reduced.

4.3. Maximum constant boost PWM with THI

The figure 10 demonstrates the sketch map of Maximum Constant Boost PWM with THI. There are five curves in this control, three reference signals V_a, V_b and V_c and two DC Voltage lines V_p and V_n. The sketch map of the third harmonic injection control method, with 1/6 of the third harmonic, is shown in Fig 10. When the carrier triangular wave greater than the upper envelope V_p or lower than

the Lower envelope V_n, the circuit turns into a shoot through state. Otherwise, it operates as a traditional PWM. As we can see, it is identical to the previous maximum constant boost control method. Therefore, the voltage gain can also be calculated by the same equation. The difference is that, the modulation index range increased to $\frac{2}{3}\sqrt{3}$. This increases the working area and the stress on the devices is reduced in this method.

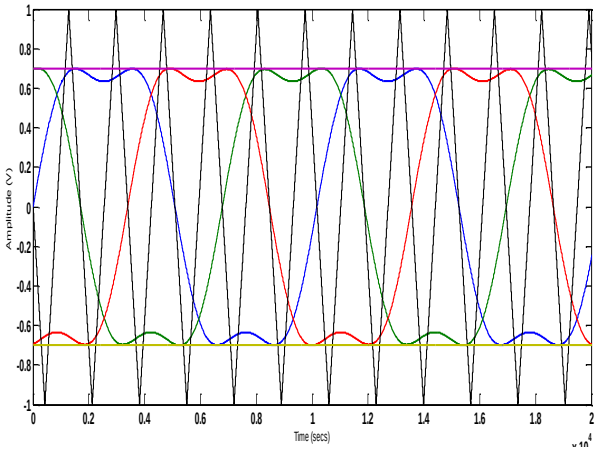


Fig. 10: Maximum Constant Boost PWM with THI.

The shoot through duty ratio can be given by

$$D_0 = \frac{2-\sqrt{3}M}{2} = 1 - \frac{\sqrt{3}M}{2} \quad (25)$$

We have modulation index

$$M = \frac{G}{\sqrt{3}G-1} \quad (26)$$

The boost factor is given by

$$B = \sqrt{3G} - 1 \quad (27)$$

The voltage gain is calculated by using M and B

$$G = MB = \frac{M}{\sqrt{3}M-1} \quad (28)$$

5. Results

Below tables shows the performance comparison of proposed topology with three different techniques for different wind velocities.

Table 1: Performance Comparison of ZSI and SL ZSI Based AFPMSG Wind Energy Conversion System at Variable Speed with Simple Boost PWM Techniques M=0.8

Wind Speed (m/s)	Generator speed (pu)	Generated Voltage(V)	Inverter Boosted Voltage		THD (%)
			ZSI	SL-ZSI	
6	0.3	116 V	160.1V	322.33 V	5.75
8	0.5	156 V	360 V	772.4 V	5.60
10	0.6	168 V	525.5 V	882.9 V	5.58
12	0.8	240 V	711.9 V	1.19K V	5.49

Table 2: Performance Comparison of ZSI and SL ZSI Based AFPMSG Wind Energy Conversion System at Variable Speed with Maximum Constant Boost PWM Techniques M=0.8

Wind Speed (m/s)	Generator speed (pu)	Generated Voltage (V)	Inverter Boosted Voltage		THD (%)
			ZSI	SL-ZSI	
6	0.3	116 V	160.1V	347.57 V	8.84
8	0.5	135 V	361.2V	904.1 V	8.57
10	0.6	168 V	528.1V	1.14K V	8.57
12	0.8	240 V	715.2 V	1.55K V	8.61

Table 3: Performance Comparison of ZSI and SL ZSI Based AFPMSG Wind Energy Conversion System at Variable Speed with Maximum Constant Boost PWM with THI Techniques M=0.8

Wind Speed (m/s)	Generator speed (pu)	Generated Voltage (V)	Inverter Boosted Voltage		THD (%)
			ZSI	SL-ZSI	
6	0.3	116 V	116.4 V	337.2 V	3.37
8	0.5	135 V	263.4 V	908.1 V	3.34
10	0.6	168 V	383.2 V	1.13K V	3.34
12	0.8	240 V	517.8 V	1.54K V	3.30

The figures shows the output results of Axial Flux Permanent Magnet Synchronous Generator based wind energy conversion system connected to grid with SL ZSI at the wind speed of 12 m/s.

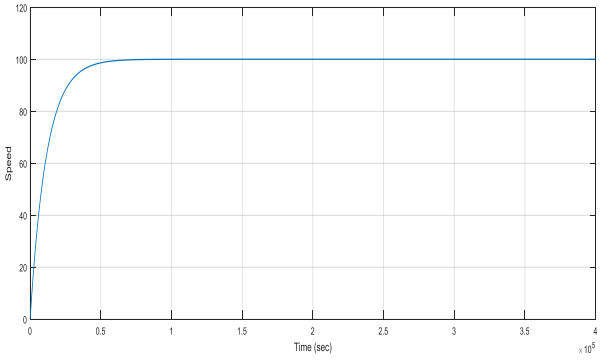


Fig. 11: Wind Turbine Speed.

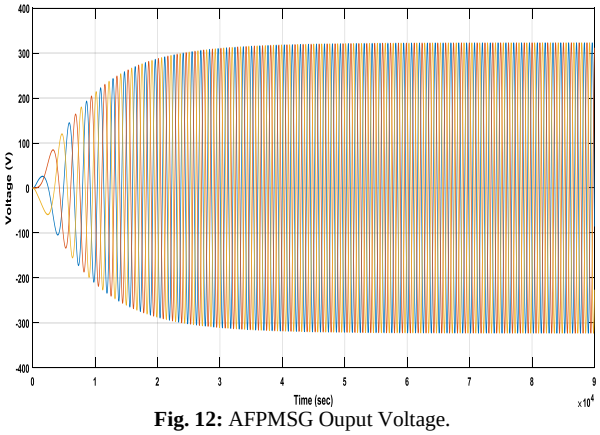


Fig. 12: AFPMSG Ouput Voltage.

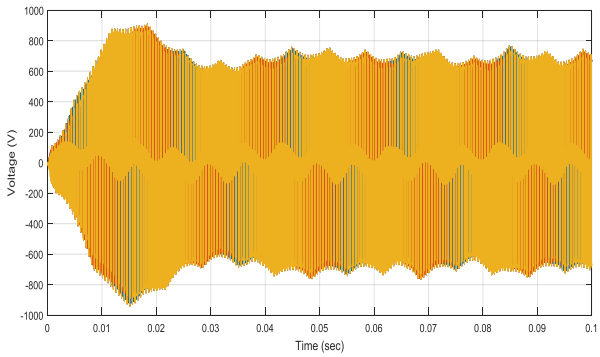


Fig. 13: Output Voltage of SL ZSI without Filters.

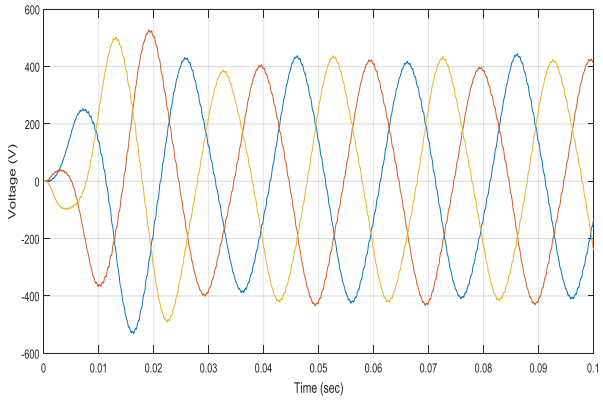


Fig. 14: Output Voltage of SL ZSI with Filters.

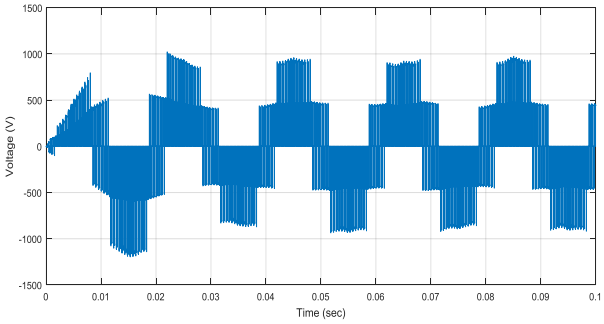


Fig. 15: Phase Voltage of SL ZSI.

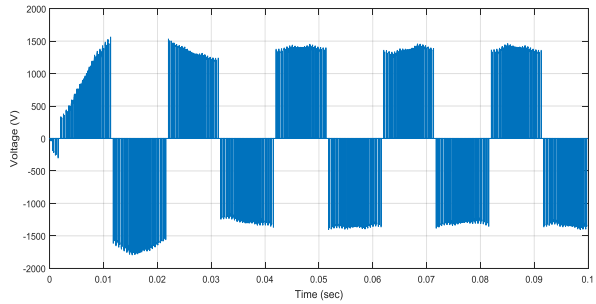


Fig. 16: Line Voltage of SL ZSI.

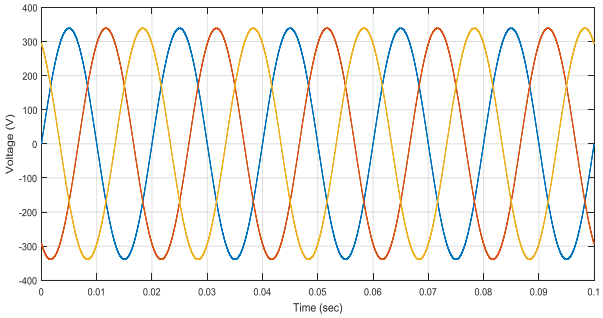


Fig. 17: Grid Voltage.

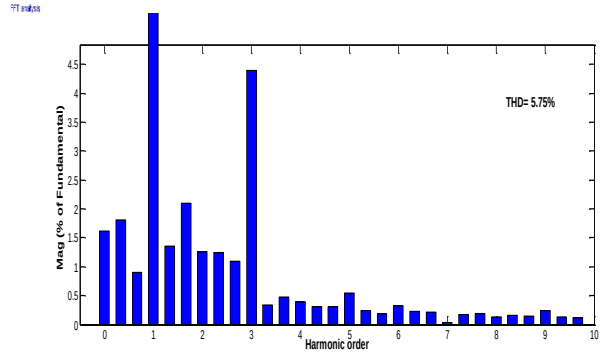


Fig. 18: Harmonic Spectrum of Output Volatge with Simple Boost PWM.

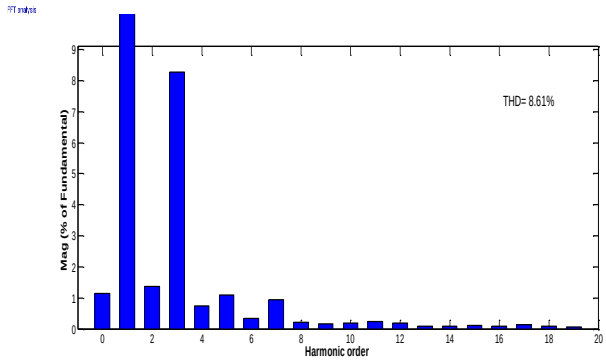


Fig. 19: Harmonic Spectrum of Output Volatge with Maximum Constant Boost PWM.

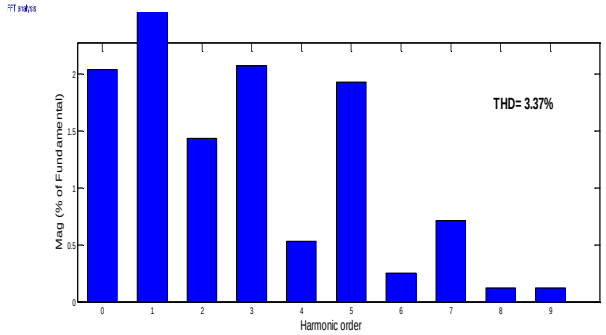


Fig. 20: Harmonic Spectrum of Output Volatge with Maximum Constant Boost PWM Using THI.

6. Conclusion

This paper explained the Performance comparisons of ZSI and SL ZSI based Axial Flux Permanent Magnet synchronous generator WECS for different wind speeds with different PWM techniques. In this, AFPMSG is modeled in MATLAB/SIMULINK in order to validate it and for the proposed inverter circuit. The SL ZSI increased the MPPT capability and reliability of ZSI based AFPMSG Wind Energy Conversion System. From the simulation results, concluded that SL ZSI boost the voltage two times more than ZSI by using the same modulation index value, and stress on the capacitors and inverter bridge is also reduced. In this, three types of Pulse Width Modulation Techniques are successfully applied to know the performance of SL ZSI. In that Maximum Constant Boost PWM gave the Maximum Boost voltage but it generates more THD, so it is not appropriate PWM technique for SL ZSI. To reduce the THD, Maximum Constant Boost PWM is implemented using THI in this paper. It gave the simple shoot through placement under varying input conditions. The ripples and the switching stresses are low.

References

[1] Ali Reza Dehghanzadeh, Vahid Behjat, Mohamad Reza Banaei "Dynamic modeling of Wind Turbine based axial flux permanent magnet synchronous generator connected to grid with switch reduced converter" Ain Shams Engineering Journal 2015

[2] V. Ramesh Babu, Dr. M.P soni, Ch. Manjeera. "Modeling of Axial Flux Induction Machine with Sinusoidal Winding Distribution" INDICON 2012 pp.481-486.

[3] Sriram S. Laxminarayan, Manik Singh, Abid H. Saifee, Arvind Mittal "Design, modeling and simulation of variable speed Axial Flux Permanent Magnet wind Generator" Sustainable Energy Technology and Assessments 19 (2017) 114-124.

[4] Omar Ellabban and Haitham Abu-Rub "Z-Source Inverter a topology improvement review" IEEE Industrial Electronics Magazine March 2016 pp 7-24.

[5] M.S Bakar, N.A Rahim, K.H.Ghazali, A.H .M. Hanafi "Z-Source Inverter Pulse Width Modulation: A survey" International Conference on Electrical, Control and computer Engineering Pahang, Malaysia, June 21-22, 2011. pp 313-316.

[6] Fang Zheng Peng, Miaosen Shen, Zhaoming Qian "Maximum Boost Control of the Z-Soure Inverter" IEEE Transaction Power Electronics Vol 20, No 4, July 2005 pp: 833-838.
[7] Miaosen Shen, Jin Wang, Alan Joseph, Fang Z.Peng, Leon M.Tolbert and Donald J Adams"Maximum Constant Boost Control of the Z-Source Inverter" IEEE 2014 pp 142-147.
[8] M. Aydin, T.A.lipo "Axial flux Permanent Magnet disc machines" WEMPEC 2017.
[9] H. Rostami, D.A. Khaburi "Voltage Gain Comparison of Different Control Methods of the Z-Source Inverter" IEEE 2007 pp I268-I272.
[10] Quoc-Nam Trinh, Hong-Hee Lee and Tae-Wonchun "A new Z-Source Inverter Topology to improve voltage boost ability" eighth International Conference on Power Electronics ECCE Asia 2011 pp 1981-1986.Huang Feng. "A Comparative Study of Legal Systems of International Financial Sanctions". Journal of Comparative Law, Vol. 3, 2012.
[11] Chen Yisheng, Ma Xin. Financial Sanctions—A New U.S. Global Asymmetric Power. China Economic Publishing House, 2015, p. 36.
[12] Wang Lei, Liu Jianwei. "The Decisions of the EU Foreign Sanctions: Systematic Design and Influencing Factors". International Review, Vol. 1, 2016.
[13] [Duan Kang. "The Financial Institutions of China and Singapore Will Be Immune to America's Sanctions against Iran Petroleum". Aerospace China, Vol. 8, 2012.